Energy Proceedings
Vol 42, 2024
ISSN 2004-2965

Influence of lubricating oil on heat transfer and pressure drop characteristics of R134a flow condensation in mini-channels

Jie Peng[1], Jianfeng Chao[2], Qifan Wang[1], Xuetao Liu[1], Minxia Li[1*], Chaobin Dang[3], Yu Zhang[1]

1 Key Laboratory of Efficient Utilization of Low and Medium Grade Energy (Tianjin University), Ministry of Education of China, Tianjin 300072, China

2 Beijing Institute of Spacecraft System Engineering, Beijing, 100094, China

3 Faculty of Engineering, Fukui University, Fukui City, 910-8507, Japan
(*Corresponding Author: tjmxli@tju.edu.cn)

ABSTRACT

In space refrigeration and heat pump systems, the presence of lubricating oil in mini-channel condensers introduces problems of reduced heat transfer efficiency and increased pressure drop. In this paper, the flow condensation of refrigerant R134a in a mini-channel under microgravity is investigated by numerical simulation, and the effects of lubricating oil on heat transfer and pressure drop are analyzed for different tube shapes, hydraulic diameters, and mass fluxes. It was found that as the lubricating oil concentration increases, the heat transfer coefficient decreases while the pressure gradient increases for the same vapor quality. This phenomenon is due to the fact that the presence of the lubricating oil increases the fluid viscosity and the viscous shear increases, leading to a reduction in the inertial forces and the relative velocity of the gas-liquid. Define the ratio of the condensation heat transfer coefficient of the oil-containing refrigerant to the condensation heat transfer coefficient of the pure refrigerant at the same operating condition as the "oil impact factor". When holding the oil concentration constant, the oil impact factor increases as the mass flow rate decreases and the channel hydraulic diameter increases. Moreover, as the refrigerant vapor quality decrease, the oil impact factor also exhibits an upward trend. This study provides optimization insights for the design and development of condensers used in space refrigeration/heat pump systems.

Keywords: mini-channel, lubricating oil, condensation, R134a, microgravity

NONMENCLATURE

Abbreviations	
c_p	Specific heat at constant pressure ($J \cdot kg^{-1} \cdot K^{-1}$)
D	Diameter (m)
F_{vol}	Volume force ($N \cdot m^{-1}$)
G	Mass flux ($kg \cdot m^{-2} \cdot s^{-1}$)
g	Gravity ($m \cdot s^{-2}$)
h_{LV}	Latent heat ($J \cdot kg^{-1}$)
k	Turbulent kinetic energy
r	Empirical coefficient (s^{-1})
S_E	Energy source item ($W \cdot m^{-3}$)
S_G	Gas phase mass source term ($kg \cdot m^{-3} \cdot s^{-1}$)
S_L	Liquid phase mass source term ($kg \cdot m^{-3} \cdot s^{-1}$)
t	Time (s)
T	Temperature (K)
We	Weber number
x	Vapor quality
y^+	Dimensionless thickness of the first layer mesh
Symbols	
ρ	*Density ($kg \cdot m^{-3}$)*
σ	*Surface tension coefficient ($N \cdot m^{-1}$)*
α	Volume fraction
λ	Thermal conductivity ($W \cdot m^{-1} \cdot K^{-1}$)
μ	Dynamic viscosity (Pa·s)
ε	Turbulent dissipation rate
κ	Curvature (m^{-1})

This is a paper for 15th International Conference on Applied Energy (ICAE2023), Dec. 3-7, 2023, Doha, Qatar.

1. INTRODUCTION

As space exploration continues to advance [1], effective heat management becomes a pressing issue. The hot environment inside spacecraft requires efficient heat dissipation, as well as refrigeration to preserve food, and biological samples, and support various scientific research. As a result, vapor compression refrigeration and heat pump systems, which are widely used in space, are becoming increasingly important. These systems play a key role in maintaining the temperature and environmental conditions inside spacecraft. In 1977, Berner et al [2] of the European Space Agency proposed a vapor compression system as a single-stage refrigeration unit on a space station to provide the required low-temperature environment for food, pharmaceuticals, and other items. Subsequently, Dexter et al [3] revealed the potential of heat pumps for large spacecraft applications by comparing a single-phase fluid-thermal control system with an electrically driven heat pump system.

In vapor compression systems, the flow condensation process plays a critical role in enabling the working medium to efficiently release heat and complete the transition from the gas phase to the liquid phase. Given the long duration and complexity of future space missions, the two-phase heat exchanger in a vapor compression refrigeration/heat pump system must be compact and efficient in heat transfer. The introduction of mini-channel heat exchanger technology in heat pump/refrigeration systems is expected to significantly increase heat exchange efficiency [4-5], reduce the refrigerant charge [6], and lower the overall weight of the system [7]. Some scholars have carried out researches on the flow condensation in mini-channel, and studied the characteristics of flow, heat transfer and pressure drop experimentally or theoretically. Ding et al. [8] conducted a visual experimental study on the flow condensation of R410A in a rectangular channel with a hydraulic diameter of 0.67mm. The study revealed that under the same conditions, the wavy flow, annular flow, intermittent flow and bubble flow appear successively in the condensation process when the mass flux is low, while the intermittent flow and bubble flow gradually disappear with the increase of the mass velocity. Chu et al. [9] proposed a novel trapezoidal drain structure to enhance the condensation heat transfer in rectangular mini-channel. The result showed that the structure can entrain the liquid film effectively through gravity and surface tension, thus increasing the contact area between vapor and wall. However, none of these studies considered the effect of lubricating oil on the flow condensation process in mini-channels.

Lubricating oils play multiple critical roles in vapor compression refrigeration systems, including reducing friction and wear, conducting heat, maintaining sealing performance, and cooling. Lubricating oil is typically collected in an oil separator or oil separation device in the system to separate the lubricating oil from the refrigerant and prevent the lubricating oil from entering critical components such as the evaporator or condenser. If the lubricating oil is not completely collected or separated, it can lead to refrigerant contamination, which can reduce system efficiency and increase maintenance requirements. However, in microgravity or zero-gravity conditions, the oil separator will not be able to rely on gravity to separate the refrigerant from the lubricating oil [10-11]. As a result, its oil separation and recovery effectiveness will be greatly reduced, causing more lubricating oil than in normal gravity conditions to enter the heat exchanger and circulate throughout the entire system. Therefore, the impact of lubricating oil on the system's heat exchange under microgravity conditions cannot be ignored. Consequently, it is crucial to study the effect of lubricating oil on the flow condensation process in mini-channels under microgravity conditions.

In this paper, the condensation process of R134a refrigerant in a mini-channel with different oil contents is numerically simulated on the basis of a refrigerant-lubricant mixture model. The effects of oil content on the flow condensation heat transfer and pressure drop were analyzed under different channel shapes, hydraulic diameters, mass flow rates and vapor masses. In addition, the effects of refrigerant vapor quality, gravity and other factors on the role of lubricating oil were investigated, and the impact factors of lubricating oil on the flow condensation heat transfer in the mini-channel under different conditions were comparatively investigated.

2. MODEL SETTING

2.1 Physical model

The research objective of this paper is the flow condensation of R134a in mini-channels, with a saturated temperature set at 40°C. The thermophysical properties of the fluid can be obtained from the REFPROP 9.1 database [12], which are temperature-dependent. R134a undergoes heat release and transitions from a saturated gas to a gas-liquid two-phase state. The mass flux of the fluid ranges from 200 to 800 kg·m^{-2}·s^{-1} (turbulence from the inlet), and the hydraulic diameter of the channel is set at 0.5, 1, and 2 mm. Geometric models include horizontal single circular channels, square channels, and regular triangular channels. The schematic diagram of the geometric models used in this paper is shown in Fig. 1. Each channel shape has the same hydraulic diameter, as illustrated in Fig. 2.

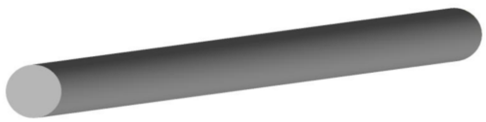

(a) Circular channel

(b) Square channel

(c) Regular triangular channel

Fig. 1 Schematic diagram of geometric models

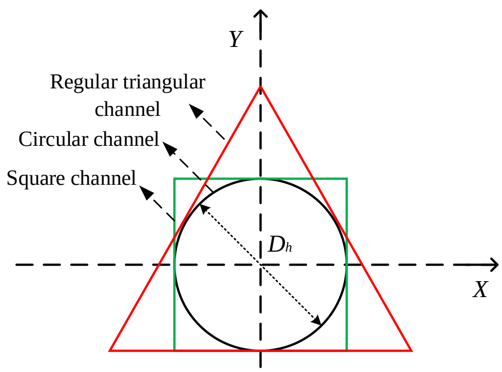

Fig. 2 Channel sections with the same hydraulic diameter and different shapes

ANSYS Fluent is adopted to perform the numerical work. The velocity boundary condition is applied to the computational domain inlet, and the pressure boundary condition is adopted at the outlet. The tube wall is set as a smooth, non-slip and non-thickness surface. On account of the existence of entrance effect [13], the adiabatic wall is set up after the inlet to allow the fluid to develop fully. Generally, the length of inlet section is about 25 to 50 times the diameter of channel, but if the inlet fluid is turbulent, the length of inlet section is about 10-15 times the diameter of channel [14]. In this study, the total length of channel is set as 130mm, in which the fluid in the first 30mm section flows adiabatically, and the condensation occurs in the last 100mm section. It is sufficient to ensure the full development of fluid at the beginning of condensation. Since the refrigerant is generally cooled by the cooling water in the condenser, and the temperature of the cooling water is approximately linearly changed with the length of flow, the heat flux on the wall of the condensation section is set to be constant.

The computational domain is filled with structured hexahedral mesh. Due to the boundary layer, the mesh is refined uniformly near the wall region and the mesh size increases gradually in the radial direction. The height of the first layer of the near-wall mesh is set to ensure y+ is less than 1. In addition, in order to speed up the simulation, on the premise of maintaining high computational accuracy, the appropriate mesh number is set in each geometric model.

2.2 Section of Introduction

2.2.1 VOF model

The VOF (Volume of Fluid) model has been proven to be an effective way to track the motion of the liquid and vapor interface between two immiscible and incompressible fluids [15]. For this model, the sum of the volume fractions of each control body item must be 1.

$$\alpha_L + \alpha_G = 1 \tag{1}$$

Since different phases share a set of momentum equation and energy equation, the VOF model treats the two-phase mixture as a single fluid, and the thermophysical properties (density, thermal conductivity, dynamic viscosity and specific internal energy) of the two-phase mixture in calculation unit can be obtained by the following formulas:

$$\rho = \rho_L \alpha_L + \rho_G \alpha_G \tag{2}$$

$$\lambda = \lambda_L \alpha_L + \lambda_G \alpha_G \tag{3}$$

$$\mu = \mu_L \alpha_L + \mu_G \mu_G \tag{4}$$

$$E = \frac{\alpha_L \rho_L E_L + (1-\alpha_L)\rho_G E_G}{\alpha_L \rho_L + (1-\alpha_L)\rho_G} \tag{5}$$

Governing equations include continuity equation, momentum equation and energy equation. The governing equations for steady state are listed as follows:

Continuity equation:

$$\nabla \cdot \left(\alpha_G \rho_G \vec{u}\right) = S_G \tag{6}$$

$$\nabla \cdot \left(\alpha_L \rho_L \vec{u}\right) = S_L \tag{7}$$

Momentum equation:

$$\nabla\cdot\left(\rho\vec{u}\vec{u}\right)=-\nabla p+\nabla\cdot\left[\mu\left(\nabla\vec{u}+\nabla\vec{u}^{T}\right)\right]+\rho\vec{g}+\vec{F}_{vol} \tag{8}$$

Energy equation:

$$\nabla\cdot\left[\vec{u}\left(\rho E+p\right)\right]=\nabla\cdot\left(\lambda_{eff}\nabla T\right)+S_E \tag{9}$$

$$\lambda_{eff}=\lambda+\frac{C_p\mu_t}{Pr_t} \tag{10}$$

2.2.2 Component Transportation Model

In refrigeration and heat pump equipment, R134a compressors typically employ POE lubricating oil (Polyolester synthetic oil) due to its good compatibility with the refrigerant. In the simulations discussed in this paper, the inlet flow consists of gaseous R134a and lubricating oil fluid. Initially, these two phases are immiscible. However, as the flow undergoes condensation and heat transfer, a portion of the gaseous R134a turns into the liquid phase and mixes with the lubricating oil. This results in a fluid that can be described as an R134a-lubricating oil mixture. Since no chemical reaction occurs between R134a and the lubricating oil during condensation, and only diffusion effects are at play, we activate the Species Transport model and configure it to represent the liquid phase as a multi-component mixture of R134a and lubricating oil.

The Species Transport model handles multi-component mixtures, which can be either fixed-component or variable-component mixtures. In the case of variable-component mixtures, changes in component concentrations can occur due to various factors like combustion, chemical reactions, or other mass transfer processes. As the liquid-phase R134a continuously increases during the condensation phase transition, our R134a-lubricating oil mixture falls into the category of variable-component mixtures. In our User-Defined Function (UDF) for the condensation phase transition, we need to direct the mass source term pointer toward the liquid-phase R134a component within the mixture. For multi-component simulations, the Species Transport model includes component equations that determine the mass fractions (Yi) of each component. These equations are solved through the convection-diffusion equation for each component.

$$\frac{\partial\left(\rho Y_i\right)}{\partial t}+\nabla\cdot\left(\rho\vec{u}Y_i\right)=-\nabla\vec{J_i}+R_i+S_i \tag{11}$$

2.2.3 Turbulence model

An appropriate turbulence model is helpful to the prediction of turbulent flow. The k-ε model has the advantages of reliability, good convergence and low demand for computer memory [16]. In this study, the realizable k-ε model is adopted, which can effectively simulate the character of turbulence on the premise of saving computing resources, and avoid the turbulent viscosity being too high predicted. Compared with the standard k-ε model, the Realizable k-ε model is improved in two parts [17]: (1) The constant coefficient is changed into a variable in the solution formula of turbulent viscosity; (2) Based on the exact equation of mean square eddy current transport, the modified transport equation of turbulent dissipation rate is derived to make it more consistent with the turbulent characteristics.

Besides, when the flow near the wall has a great influence on the whole flow or the Re number is low, the enhanced wall treatment has the best effect. In the process of flow condensation, the liquid film will be produced at the wall, which will reduce the Re number near the wall. Therefore, the enhanced wall treatment method is adopted in the simulation.

2.2.4 Surface tension model

To take into account the effects of surface tension, the CSF (Continuum Surface Force) model proposed by Brackbill et al. [18] is adopted. Then the surface force can be expressed as a volume force in the momentum equation, which is computed as follows:

$$\vec{F}=\sigma\frac{2\rho\kappa_L\nabla\alpha_L}{\rho_L+\rho_G} \tag{12}$$

The divergence of the unit surface normal at the interface can be used to compute the surface curvature:

$$\kappa_L=\nabla\cdot\frac{\nabla\alpha_L}{\left|\alpha_L\right|} \tag{13}$$

2.2.5 Phase change model

Lee model [19] is a simplified evaporation-condensation model, in which the main driving force of phase change is the temperature difference between the temperature and saturation temperature of each cell in the computational domain. The larger the temperature difference, the faster the rate of phase change. In this study, the Lee model is adopted to simulate the condensation process by adding the following equations to the governing equations as a source term through the user defined functions:

$$S_G=-S_L=\begin{cases} r\alpha_G\rho_G\dfrac{\left(T-T_{sat}\right)}{T_{sat}}, & \text{if } T\le T_{sat} \\ r\alpha_L\rho_L\dfrac{\left(T-T_{sat}\right)}{T_{sat}}, & \text{if } T\ge T_{sat} \end{cases} \tag{14}$$

$$S_E = S_L h_{LV} \quad (15)$$

Where r is the empirical coefficient [20], which is actually associated with the fluid, geometry, boundary conditions and even mesh size [21]. Riva et al. [22] found that too small value of r would lead to a large difference between the temperature of the gas-liquid interface and the saturation temperature, while too large value of r would make the simulation calculation difficult to converge. In this paper, the value of r is adjusted by trial-and-error method, which increases from 5×10^5 to 1.5×10^6 s^{-1} with the increase of mass flux to ensure that the difference between the gas-liquid interface temperature and saturation temperature is less than 1 K.

2.3 Material Properties

For the R134a refrigerant, a saturation temperature of 40°C was selected, and the thermophysical properties of each phase can be queried by REFPROP 10.0 and filled in the material interface. Tab. 1 demonstrates the comparison of each thermophysical property between POE lubricating oil and R134a gas-liquid two-phase under simulated working conditions. It should be noted that the kinetic viscosity of the lubricating oil is much higher than that of the liquid R134a, and its surface tension coefficient is also higher, so due to the difference in physical properties, the lubricating oil will inevitably have some influence on the heat transfer and pressure drop characteristics of the refrigerant.

Tab. 1
Under simulated operating conditions, the thermophysical parameters of POE lubricating oil and R134a are examined.

Parameters	POE	Saturated liquid R134a	Saturated gaseous R134a
ρ / kg·m^{-3}	942.0	1147	50.09
Cp / J·kg^{-1}·K^{-1}	1872	1498	1145
λ / W·m^{-1}·K^{-1}	0.1198	0.0747	0.0154
μ / Pa·s	0.0619	1.615e-4	1.237e-05
σ / N·m^{-1}	0.0274	6.115e-3	-

2.4 Model validation

In simulation calculations, the density of the mesh has a direct impact on the accuracy of the results. In general, the denser the mesh, the more accurate the simulation results are, but this is also accompanied by an increase in the amount of computation as well as an increase in the time required for computation, which will greatly consume computer resources [23]. Therefore, using a circular channel (D_h = 1 mm) with 1% oil content as an example, we performed a grid-independent validation as shown in Fig. 3. There is only a 1.3% difference in the average heat transfer coefficient using 5.9 million meshes compared to the case using 4.3 million meshes. Therefore, we determined that the use of 4.3 million meshes is appropriate in this case.

Fig. 4 compares the simulation data with the experimental data by Huang et al. [24] for the condensation heat transfer coefficient in a horizontal circular channel (D_h=1.6 mm) at mass flux of 500 kg·m^{-2}·s^{-1}. The result shows that in that case, the relative errors between the simulated data and the experimental data are within 11.6%, which indicates the reliability and accuracy of the numerical model in this study.

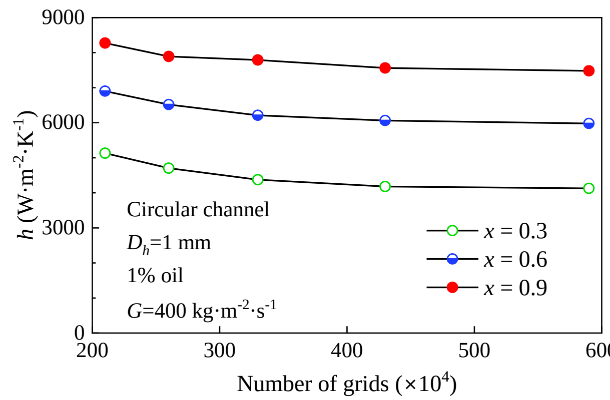

Fig. 3 Average heat transfer coefficient with different mesh numbers

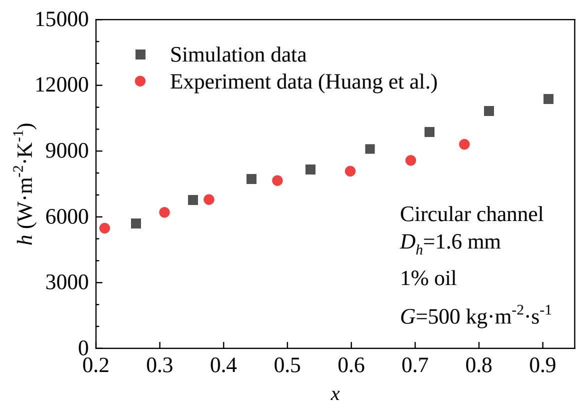

Fig. 4 Comparison of simulation data, experimental data and correlation of condensation heat transfer coefficient

3. RESULTS

This section conducts a study on the impact of lubricating oil concentration on the condensing heat transfer coefficient of R134a based on the modeling of refrigerant-lubricant mixtures. It should be noted that, in this study, oil concentration is defined as the ratio of the lubricant's mass flow rate to the total mass flow rate.

3.1 Influence of lubricating oil on flow condensing heat transfer characteristics

The variation of condensation heat transfer coefficients with vapor quality for R134a containing different oil concentrations in three types of channels is depicted in Fig. 5. The channels have a hydraulic diameter of 1 mm, and a mass flow rate of 400 kg·m^{-2}·s^{-1}, and the studied oil concentrations are 0% (pure working fluid), 1%, and 5%, respectively. As shown in the figure, the condensation heat transfer coefficient decreases as vapor quality decreases in the case of working fluid containing oil. This trend aligns with the behavior observed in pure R134a condensation heat transfer and is attributed to the thickening of the condensate film. Lubricating oil has a detrimental effect on R134a condensation heat transfer, and the higher the oil concentration, the lower the condensation heat transfer coefficient at the same vapor quality. This is because the viscosity of the lubricating oil is significantly higher than that of the refrigerant, leading to the formation of an oil film on the wall at high vapor quality, increasing heat transfer resistance. In the mixed liquid film at low vapor quality, even though the mass ratio of lubricating oil is smaller than that of R134a, the overall viscosity of the liquid film is still higher compared to the pure industrial liquid film. Consequently, this reduces the average velocity of the liquid phase and turbulence intensity, thus deteriorating the condensation heat transfer.

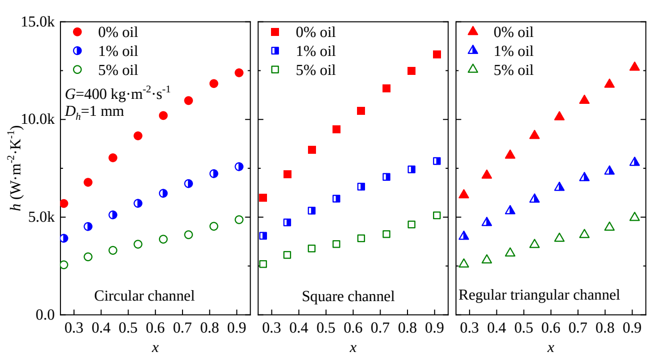

Fig. 5 Influence of lubricating oil concentration on condensation heat transfer coefficient in channels of three shapes

Fig. 5 Influence of lubricating oil concentration on condensation heat transfer coefficient in channels of three shapes

As the vapor quality decreases, the local oil concentration of the lubricating oil in the liquid-phase mixture gradually decreases, and the overall viscosity also decreases. Consequently, the trend of the heat transfer coefficient decreasing with vapor quality becomes slower. Furthermore, unlike the case of pure vapor condensation, there is little difference in the heat transfer coefficients for condensation of oil-containing working fluid in the three passages. This indicates that the oil film is less affected by surface tension, is more uniformly distributed on the wall, and contributes to a larger thermal resistance, significantly influencing the overall heat transfer.

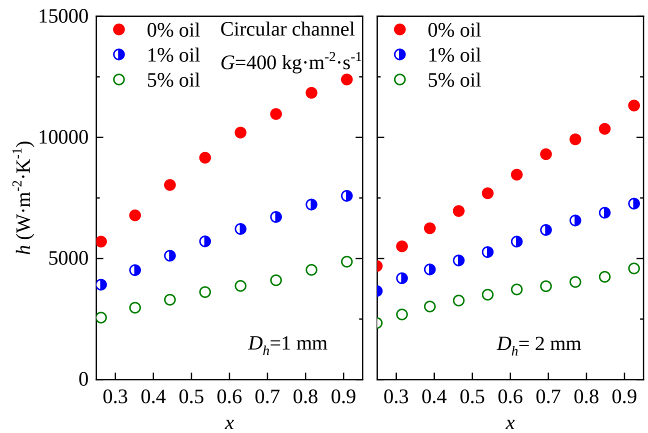

Fig. 6 Influence of lubricating oil concentration on condensation heat transfer coefficient in channels with different hydraulic diameters

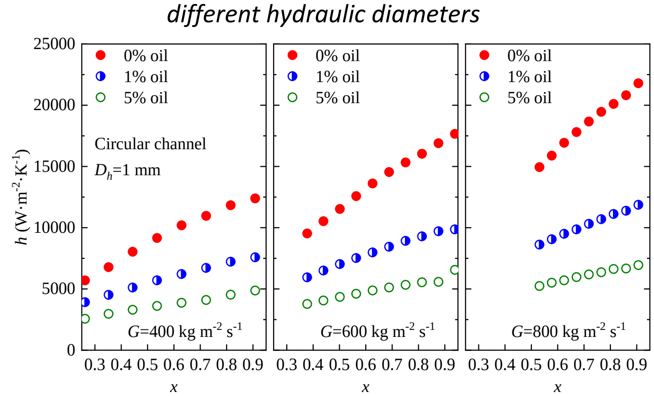

Fig. 7 Influence of lubricating oil concentration on condensation heat transfer coefficient at different mass fluxes

Fig. 6 depicts the variation of the condensation heat transfer coefficient with vapor quality for oil-laden R134a at different hydraulic diameters in a circular channel, with a mass flow rate of 400 kg·m^{-2}·s^{-1}. As shown in the graph, in the absence of oil, the condensation heat transfer coefficient significantly decreases as the hydraulic diameter increases. However, at 1% and 5% oil concentrations, the reduction in heat transfer coefficient is minimal and can be practically neglected. This observation suggests that the influence of surface tension on the R134a-oil liquid film is more significant than on the pure R134a liquid film under the same conditions, resulting in a lesser impact of hydraulic diameter changes on the former's liquid film distribution.

Fig. 7 shows the variation of condensation heat transfer coefficient with vapor quality at different mass flow rates for oil-containing R134a with different oil concentrations in a circular channel with a hydraulic diameter of 1 mm. It can be found that, compared with oil-containing working fluid, pure R134a shows a greater enhancement of the condensation heat transfer coefficient through the increase of mass flow rate, due to the viscosity of the lubricating oil, and the oil-containing fluid film relative to the overall mass flow rate increase. The increase in flow rate is limited, resulting in a smaller increase in heat transfer coefficient with increasing mass flow rate.

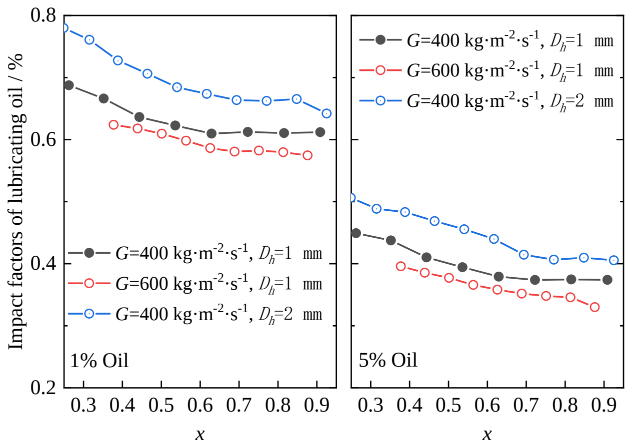

Fig. 8 Variation of impact factors of lubricating oil with different concentrations on condensation heat transfer coefficient with vapor quality

Based on the analysis provided, it's clear that the presence of lubricating oil in miniature channels adversely affects the condensation heat transfer of R134a. This heat transfer deterioration varies depending on the oil concentration. We define the oil impact factor as the ratio of the condensation heat transfer coefficient for oil-containing working fluid to that of pure working fluid under identical conditions. This factor quantifies the extent to which lubricating oil hampers the condensation heat transfer. Fig. 8 depicts the lubricating oil influence coefficient versus vapor mass for different lubricating oil concentrations, taking into account variations in hydraulic diameter and mass flow rate. Notably, the oil impact factor consistently remains below 1, indicating a detrimental effect of lubricating oil on condensation heat transfer under these conditions. Higher oil concentrations result in lower oil impact factors, highlighting a more pronounced negative impact of lubricating oil on the heat transfer coefficient. At a 1% oil concentration, the oil impact factor ranges from 0.58 to 0.78, while at a 5% oil concentration, it varies within the range of 0.34 to 0.51.

When compared at the same oil concentration, the oil impact factor decreases with the increase of mass flow rate and increases with the increase of channel hydraulic diameter. In addition, there is a tendency for the oil impact factor to increase with decreasing vapor quality. This trend can be attributed to the gradual decrease in the local oil concentration in the liquid phase, resulting in a decrease in its viscosity. As a result, the deteriorating effect of the lubricating oil on the condensation heat transfer of the working fluid gradually diminishes. It is evident that the lubricating oil in the mini-channel has a significant detrimental effect on the condensation heat transfer of the refrigerant.

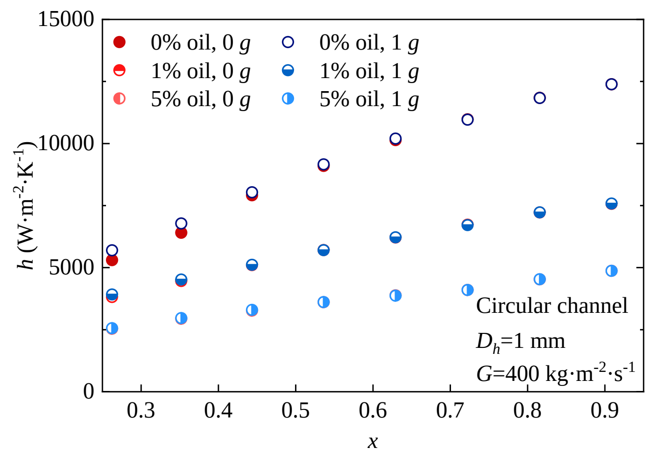

Fig. 9 Influence of lubricating oil concentration on condensation heat transfer coefficient with and without gravity

Considering that the lubricating oil in the heat pump under microgravity conditions will be difficult to avoid circulating throughout the system and affecting the performance of the heat exchanger, Fig. 9 demonstrates the effect of lubricating oil concentration on the condensation heat transfer coefficient of R134a with and without gravity conditions, in which the channel shape is circular, the hydraulic diameter is 1 mm, and the mass flow rate is 400 kg·m^{-2}·-s^{-1} For the pure workpiece, the gravity-free conditions are not suitable for the condensation heat transfer coefficient of the R134a due to liquid film uniform distribution, its condensation heat transfer coefficient is significantly lower compared to the normal gravity condition. For 1% and 5% oil concentration of oil-containing workpiece, gravity has basically no effect on condensation heat transfer, which is because the surface tension coefficient of oil-containing workpiece is higher, and the effect of surface tension weakens the effect of gravity on condensation heat transfer. Therefore, in engineering design, the heat transfer correlation equation for condensation of oil-containing working fluid under normal gravity conditions can more accurately predict the heat transfer characteristics under microgravity conditions compared with pure refrigerant.

3.2 Influence of lubricating oil on flow condensing pressure drop characteristics

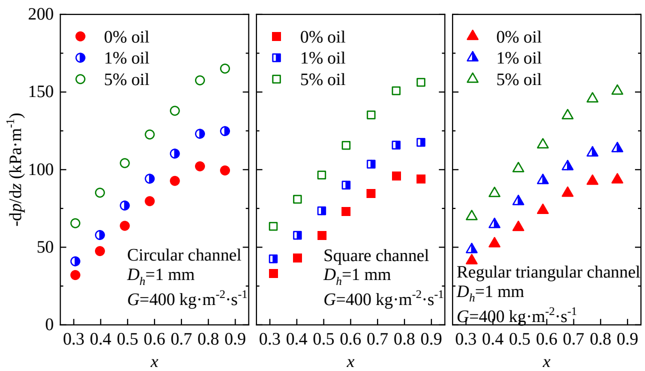

Fig. 10 Influence of lubricating oil concentration on condensation pressure drop gradient in channels of three shapes

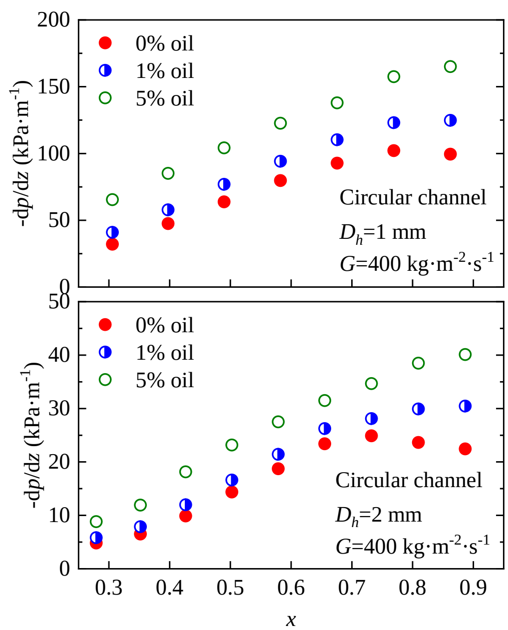

Fig. 11 Influence of lubricating oil concentration on condensation pressure drop gradient in channels with different hydraulic diameters

Fig. 10 illustrates how the pressure drop gradient changes as vapor quality varies for R134a mixed with oil at different concentrations in various channel shapes. These channels have a 1 mm hydraulic diameter and a mass flow rate of 400 kg·m^{-2}·s^{-1}. In general, the pressure drop gradient during condensation decreases as vapor quality decreases, similar to what's observed with pure condensation. However, at lower oil concentrations, the gradient first increases slightly and then decreases. Conversely, at higher oil concentrations, the gradient keeps decreasing. This happens because a high vapor quality oil film forms on the channel wall with more oil concentration. This film prevents direct contact between the R134a gas and the channel wall. Due to the oil film's high viscosity, it creates strong shear forces at the interfaces between the gas phase and the oil film, and between the oil film and the wall. This initially results in a higher pressure drop gradient during the early stages of condensation. But as the condensate film thickens, the relative speed between the gas and liquid decreases. This reduces the local oil concentration and lowers the overall viscosity of the liquid film, leading to a continuous decrease in the pressure drop gradient during condensation.

In addition, the gradient of condensation pressure drop of oil-containing R134a increases with increasing oil concentration. This increase is mainly due to the increase in the viscosity of the liquid-phase mixture as a result of the elevated oil concentration, which in turn promotes an increase in turbulent shear. It is worth noting that the pressure drop gradient in the circular channel is larger than the other two shapes under high vapor quality conditions. This difference in pressure drop gradient becomes more pronounced with increasing oil concentration. The main reason for this difference is the behavior of the liquid film in the square and triangular channels, which are affected by surface tension and tend to accumulate at the corners. The surface tension coefficient of the lubricating oil is relatively high and the effect of surface tension is exacerbated by increasing lubricating oil concentration. This in turn inhibits the growth of shear forces between the fluid and the wall.

The variation of the condensation pressure drop gradient with vapor quality for oil-containing R134a, with different oil concentrations, in circular channels of varying hydraulic diameters is presented in Fig. 11. The mass flow rate is set at 400 kg·m^{-2}·-s^{-1}. As observed in the figures, the increase in condensation pressure drop gradient with rising oil concentration diminishes as the hydraulic diameter increases. This phenomenon can be attributed to the fact that an increase in oil concentration elevates the surface tension coefficient of the liquid-phase mixture. Consequently, the specific gravity of the surface tension effect becomes more pronounced, particularly in larger diameter channels. This enhanced effect effectively dampens the increase in shear forces between the fluid and the channel wall.

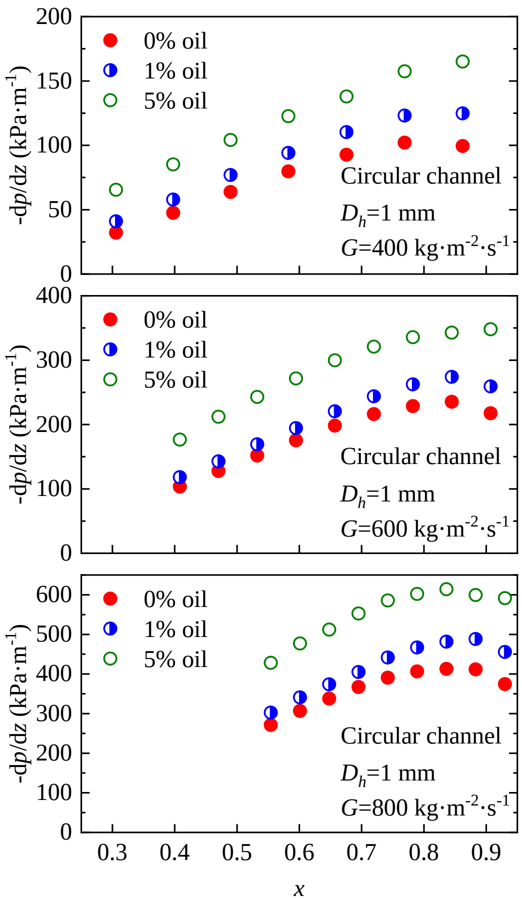

Fig. 12 Influence of lubricating oil concentration on condensation pressure drop gradient under different mass fluxes

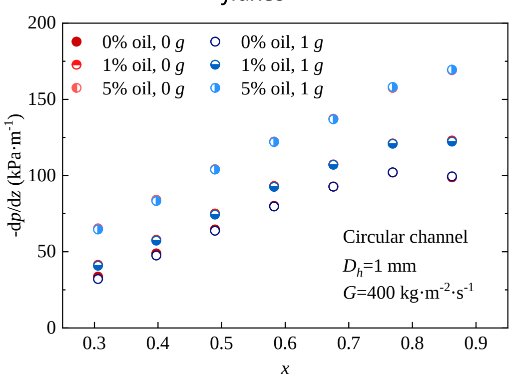

Fig. 13 Influence of lubricating oil concentration on condensation pressure drop gradient with and without gravity

Fig. 12 depict the variation of the condensation pressure drop gradient with vapor quality for oil-containing R134a at different oil concentrations in a circular channel, with varying mass flow rates. The hydraulic diameter of the channel is set at 1 mm. As the mass flow rate increases, the condensation pressure drop gradient at the same oil concentration undergoes a transition from a trend of decreasing with decreasing vapor quality to a trend of initially increasing slightly and then decreasing again. This transition suggests that, under high vapor quality conditions, the oil film distributed along the channel wall gradually becomes thinner with the increasing mass flow rate, thereby enhancing the contact between the gas phase and the channel wall.

Fig. 13 illustrates the impact of lubricating oil concentration on the condensation pressure drop gradient of R134a under both gravity and gravity-free conditions. In this scenario, the channel shape is circular, with a hydraulic diameter of 1 mm, and the mass flow rate is set at 400 kg·m^{-2}·-s^{-1}. It is noticeable that the condensation pressure drop gradient under gravity-free conditions is slightly higher compared to that under normal gravity conditions. This increase can be attributed to the rise in relative velocity between the gas and liquid phases in the absence of gravity. Furthermore, when comparing the oil-containing working fluid with the pure working fluid, the higher surface tension of the oil-containing mixture mitigates the influence of gravity. As a result, there is minimal difference in the condensation pressure drop gradient between the conditions with and without gravity.

In summary, the condensation heat transfer coefficient is primarily influenced by the thickness of the liquid film and the inertia force, while the pressure gradient is mainly affected by the viscous shear force. As the fluid flow rate increases, both the inertia force and viscous shear force rise, leading to an increase in both heat transfer coefficient and pressure drop gradient. An increase in the viscosity of the working fluid primarily amplifies the viscous shear force, while concurrently reducing the inertial force and the flow rate of the gas-liquid phases. Consequently, this results in an elevated pressure drop gradient and a reduction in the heat transfer coefficient. Therefore, the effect of lubricating oil on the channel's flow condensation heat transfer coefficient and pressure drop gradient is counteractive in nature.

4. CONCLUSIONS

This paper presents a simulation study on the influence of lubricating oil in miniature channels on R134a flow condensation heat transfer and pressure drop characteristics, based on the establishment of a refrigerant-lubricant oil mixture model. The study explores the impact of factors such as vapor quality, channel shape, mass flow rate, hydraulic diameter, and gravity on the lubricating oil effect. The following conclusions have been drawn:

(1) Lubricating oil has contrasting effects on the flow condensation heat transfer coefficient and pressure drop gradient within the channel. Higher oil concentrations result in lower condensation heat transfer coefficients at the same vapor quality level and larger pressure drop gradients.

(2) An 'oil impact factor' is defined as the ratio of the condensation heat transfer coefficient of the oil-containing medium to that of the pure medium under identical conditions. At the same oil concentration, the oil impact factor decreases with increasing mass flow rate and increases with a larger channel hydraulic diameter. Additionally, the oil impact factor tends to increase as vapor quality decreases.

(3) At low oil concentrations, the condensation pressure drop gradient exhibits a slight increase followed by a decrease, while at high oil concentrations, the pressure drop gradient consistently decreases. This behavior is linked to the high-viscosity nature of the oil film along the channel wall.

ACKNOWLEDGEMENT

This research was supported by National Natural Science Foundation of China (No. 51876135).

DECLARATION OF INTEREST STATEMENT

The authors declare that we have no known competing financial interests or personal relationships that could have appeared to influence the work reported in this paper. All authors read and approved the final manuscript.

REFERENCE

[1] Thirsk, R., Kuipers, A., Mukai, C., & Williams, D. (2009). The space-flight environment: the International Space Station and beyond. Cmaj, 180(12), 1216-1220.

[2] Berner, F., & SAVAGE, C. (1981, June). Development of a vapor compression heat pump for space use. In 16th Thermophysics Conference (p. 1113).

[3] Dexter, P., & Haskin, W. (1757). Analysis of heat pumped augmented systems for spacecraft thermal control. In 19th Thermophysics Conference (p. 1757).

[4] Kandlikar, S. G. (2002). Two-phase flow patterns, pressure drop, and heat transfer during boiling in minichannel flow passages of compact evaporators. heat transfer engineering, 23(1), 5-23.

[5] Wilk, J. (2020). Heat/mass transfer analogy in the case of convective fluid flow through minichannels. International Journal of Thermal Sciences, 156, 106467.

[6] Zhang, N., Lu, Y., Ouderji, Z. H., & Yu, Z. (2023). Review of heat pump integrated energy systems for future zero-emission vehicles. Energy, 127101.

[7] Zhao, G., Wang, X., Negnevitsky, M., & Li, C. (2023). An up-to-date review on the design improvement and optimization of the liquid-cooling battery thermal management system for electric vehicles. Applied Thermal Engineering, 219, 119626.

[8] Ding, Y., & Jia, L. (2017). Study on flow condensation characteristics of refrigerant R410a in a single rectangular micro-channel. International Journal of Heat and Mass Transfer, 114, 125-134.

[9] Chu, W. X., Chen, C. Y., Liao, Y. H., & Wang, C. C. (2019). A novel micro-channel heat sink with trapezoid drainage for enhancing condensation heat transfer of dielectric fluid. Experimental Thermal and Fluid Science, 106, 11-24.

[10] Ye, Y., Ma, R., Ning, Y., & Wu, Y. (2023). Simulation of refrigerant-lubricant two-phase flow characteristics and performance test in space compressor. Applied Thermal Engineering, 224, 120105.

[11] Peng, H., Shangguan, L., & Zhang, H. (2022). Device for Simulating Fluid Microgravity Environment Based on Magnetic Compensation Method and Research on Magnetic Fluid Lubrication Performance of Oil Film Bearing. Advances in Materials Science and Engineering, 2022, 1-13.

[12] Lemmon, E. W., Huber, M. L., & McLinden, M. O. (2002). NIST reference fluid thermodynamic and transport properties–REFPROP. NIST standard reference database, 23(2002), v7.

[13] Gamrat, G., Favre-Marinet, M., & Asendrych, D. (2005). Conduction and entrance effects on laminar liquid flow and heat transfer in rectangular microchannels. International Journal of Heat and Mass Transfer, 48(14), 2943-2954.

[14] Heikal, M. R. F., Walklate, P. J., & Hatton, A. P. (1977). The effect of free stream turbulence level on the flow and heat transfer in the entrance region of an annulus. International Journal of Heat and Mass Transfer, 20(7), 763-771.

[15] Sun, D. L., Xu, J. L., & Wang, L. (2012). Development of a vapor–liquid phase change model for volume-of-fluid method in FLUENT. International Communications in Heat and Mass Transfer, 39(8), 1101-1106.

[16] Chen, Q., Moser, A., & Huber, A. (1990). Prediction of buoyant, turbulent flow by a low Reynolds number ke model.

[17] El-Amin, M. F., Sun, S., Heidemann, W., & Müller-Steinhagen, H. (2010). Analysis of a turbulent buoyant

confined jet modeled using realizable k–ε model. Heat and mass transfer, 46, 943-960.
[18] Brackbill, J. U., Kothe, D. B., & Zemach, C. (1992). A continuum method for modeling surface tension. Journal of computational physics, 100(2), 335-354.
[19] Lee, W. H. (1980). Pressure iteration scheme for two-phase flow modeling. IN" MULTIPHASE TRANSPORT: FUNDAMENTALS, REACTOR SAFETY, APPLICATIONS"., 407-432.
[20] Wen, J., Gu, X., Wang, S., Li, Y., & Tu, J. (2018). Numerical investigation on condensation heat transfer and pressure drop characteristics of R134a in horizontal flattened tubes. International Journal of Refrigeration, 85, 441-461.
[21] Lee, H., Kharangate, C. R., Mascarenhas, N., Park, I., & Mudawar, I. (2015). Experimental and computational investigation of vertical downflow condensation. International Journal of Heat and Mass Transfer, 85, 865-879.
[22] Da Riva, E., Del Col, D., Garimella, S. V., & Cavallini, A. (2012). The importance of turbulence during condensation in a horizontal circular minichannel. International Journal of Heat and Mass Transfer, 55(13-14), 3470-3481.
[23] Wen, J., Gu, X., Wang, S., Li, Y., & Tu, J. (2018). The comparison of condensation heat transfer and frictional pressure drop of R1234ze (E), propane and R134a in a horizontal mini-channel. International Journal of Refrigeration, 92, 208-224.
[24] Huang, X., Ding, G., Hu, H., Zhu, Y., Peng, H., Gao, Y., & Deng, B. (2010). Influence of oil on flow condensation heat transfer of R410A inside 4.18 mm and 1.6 mm inner diameter horizontal smooth tubes. International journal of refrigeration, 33(1), 158-169.